

RECEIVED: May 25, 2022

REVISED: June 7, 2022

ACCEPTED: June 8, 2022

PUBLISHED: July 8, 2022

Natural mass hierarchy among three heavy Majorana neutrinos for resonant leptogenesis under modular A_4 symmetry

Dong Woo Kang,^a Jonguk Kim,^{a,1} Takaaki Nomura^b and Hiroshi Okada^{c,d}

^a*School of Physics, KIAS,
Seoul 02455, Republic of Korea*

^b*College of Physics, Sichuan University,
Chengdu 610065, China*

^c*Asia Pacific Center for Theoretical Physics (APCTP) — Headquarters San 31,
Hyoja-dong, Nam-gu, Pohang 790-784, Republic of Korea*

^d*Department of Physics, Pohang University of Science and Technology,
Pohang 37673, Republic of Korea*

E-mail: dongwookang@kias.re.kr, jkkim@kias.re.kr, nomura@scu.edu.cn,
hiroshi.okada@apctp.org

ABSTRACT: It is clear that matter is dominant in the Universe compared to antimatter. We call this problem baryon asymmetry. The baryon asymmetry is experimentally determined by both cosmic microwave background and big bang nucleosynthesis measurements. To resolve the baryon number asymmetry of the Universe as well as neutrino oscillations, we study a radiative seesaw model in a modular A_4 symmetry. Degenerate heavy Majorana neutrino masses can be naturally realized in an appropriate assignments under modular A_4 with large imaginary part of modulus τ , and it can induce measured baryon number via resonant leptogenesis that is valid in around TeV scale energy theory. We also find that the dominant contribution to the CP asymmetry arises from $\text{Re}[\tau]$ through our numerical analysis satisfying the neutrino oscillation data.

KEYWORDS: Baryo-and Leptogenesis, Cosmology of Theories BSM, Sterile or Heavy Neutrinos

ARXIV EPRINT: [2205.08269](https://arxiv.org/abs/2205.08269)

¹Corresponding author.

Contents

1	Introduction	1
2	Model	3
2.1	Majorana mass matrix	3
2.2	Inert scalar boson mass matrices	4
2.3	Neutrino sector	5
3	Resonant leptogenesis	6
4	Numerical analysis	7
5	Conclusion and discussion	11
A	Formulas in modular A_4 framework	12

1 Introduction

Understanding the origin of the observed imbalance in baryonic matter remains one of the important problems, so-called Baryon Asymmetry of the Universe (BAU) problem, in particle physics and cosmology. The baryon abundance at present Universe obtained from Cosmic Microwave Background anisotropy and Big Bang Nucleosynthesis is [1]

$$\Omega_B h^2 = 0.0223 \pm 0.0002. \quad (1.1)$$

This is related to the baryon asymmetry which is given by

$$Y_B \equiv \frac{n_B}{s} \simeq 0.86 \times 10^{-10}, \quad (1.2)$$

where n_B is the number density of the baryon and s is entropy density.

Theoretically resolving the BAU is one of the important motivations to consider physics beyond the Standard Model (SM).¹ One attractive scenario is leptogenesis [4] that is intimately related to smallness of neutrino masses through canonical seesaw mechanism [5–8] by introducing heavy Majorana fermions. The decay of the heavy Majorana neutrino creates lepton asymmetry and it is converted into baryon asymmetry by sphalerons around electroweak scale. In order to generate observed baryon asymmetry in eq. (1.2), we need

¹Even though there exists electroweak baryogenesis [2] within the context of SM, it would be almost ruled out due to requirement of too strong first order electroweak phase transition. Non-thermal WIMP baryogenesis is one of the fascinating mechanisms since re-annihilation of dark matter provides the observed baryon asymmetry as well as the correct relic density [3].

rather large mass of the Majorana neutrinos that is 10^{10} GeV at least. It implies that such heavy fermions could not be produced by any current collider experiments.

On the contrary, resonant leptogenesis [9, 10] is one of the promising candidates to explain BAU at low energy scale that could be around TeV scale being within the reach of current or near future experiments. In order to realize the resonant leptogenesis, we need two almost degenerate Majorana fermions at least.² Then, we have an enhancement of the CP asymmetry parameter [11] that can generate enough BAU even at low energy scale. The next task would be how to realize the almost degenerate masses, even though most of the endeavors set such a situation by hand unless symmetries are introduced.

Recently, a modular flavor symmetry was proposed in refs. [12, 13]. The symmetry has additional quantum number that is called modular weight, and flavor structures of dimensionless couplings such as Yukawas are uniquely determined once the modular weights are fixed. As a result, more predictive models are possible compared to traditional flavor models. In fact, a plethora of scenarios have been studied after this idea up to now, especially applying modular A_4 symmetry [12, 14–66].³ More interestingly on the resonant leptogenesis, *two degenerate Majorana fermion masses are arisen at two fixed points of modulus $\tau = i, i\infty$, once we assign three Majorana fermions N^c to be triplet under A_4 with -1 modular weight!* These fixed points are statistically favored in the flux compactification of Type IIB string theory [77].⁴ Under the assignment, the Majorana mass matrix (M_N) is given by

$$M_N = M_0 \begin{bmatrix} 2y_1 & -y_3 & -y_2 \\ -y_3 & 2y_2 & -y_1 \\ -y_2 & -y_1 & 2y_3 \end{bmatrix}, \quad (1.3)$$

where $Y_3^{(2)} \equiv (y_1, y_2, y_3)$ is A_4 triplet modular form with two modular weights appearing in Majorana mass term $\frac{1}{2}M_0 Y_3^{(2)} \overline{N^c} N$; concrete forms of modular forms are found in appendix. In the limit of $\tau = i$, we have $(0, M_0, M_0)$ mass eigenvalues after the diagonalization of eq. (1.3) [43]. The deviation from the $\tau = i$ gives small mass splitting of the two massive Majorana fermions as well as the small mass eigenvalue for the massless Majorana fermion. We naturally get the small mass splitting between two massive Majorana fermions but it is hard to realize resonant leptogenesis with one light (almost massless) Majorana fermion. In the limit of $\tau = i\infty$, on the other hand, we have $(M_0, M_0, 2M_0)$ mass eigenvalues, i.e. three heavy Majorana fermions with two degenerated one. And the deviation along the $\text{Im}[\tau]$ direction from the $\tau = i\infty$ provides small mass splitting of the lightest two massive Majorana fermions, while the deviation along the $\text{Re}[\tau]$ direction provides the CP asymmetry [78].

In this paper, we apply the modular A_4 symmetry with rather large $\text{Im}[\tau]$ to a supersymmetric radiative seesaw model, and discuss how to realize the neutrino oscillation data and BAU simultaneously [79].⁵ Radiative seesaw model [82] is known as a promising

²More concretely, the maximum enhancement may be achieved if the mass splitting between two Majorana fermions is comparable to the decay width of either Majorana fermions.

³Here, we provide useful review references for beginners [68–76].

⁴Generally, there are three fixed points adding $\tau = e^{2\pi i/3}$. But this point does not give degenerated masses under the same assignment.

⁵BAU is also discussed in modular symmetric models, e.g. in refs. [26, 46, 56, 67, 80, 81].

	Matter super fields							
Fields	$(\hat{L}_e, \hat{L}_\mu, \hat{L}_\tau)$	$(\hat{e}^c, \hat{\mu}^c, \hat{\tau}^c)$	\hat{N}^c	\hat{H}_1	\hat{H}_2	$\hat{\eta}_1$	$\hat{\eta}_2$	$\hat{\chi}$
$SU(2)_L$	2	1	1	2	2	2	2	1
$U(1)_Y$	$\frac{1}{2}$	-1	0	$\frac{1}{2}$	$-\frac{1}{2}$	$\frac{1}{2}$	$-\frac{1}{2}$	0
A_4	$\{1, 1', 1''\}$	$\{1, 1'', 1'\}$	3	1	1	1	1	1
$-k$	$\{-2, -2, 0\}$	$\{-2, -2, 0\}$	-1	0	0	-3	-3	-3

Table 1. Matter chiral superfields and their charge assignments under $SU(2)_L \times U(1)_Y \times A_4$, where $-k$ is the number of modular weight.

candidate to explain the neutrino oscillation data at low energy scale, and connect the neutrinos and dark matter or new particles. Moreover, several interesting flavor physics such as lepton flavor violations (LFVs) potentially come into our discussion. Due to almost two degenerate Majorana fermions, the resonant leptogenesis is naturally realized and proper field assignments for modular weight assure the radiative seesaw model instead of an ad-hoc symmetry such as Z_2 that is introduced by hand.

Our manuscript is organized as follows. In section 2, we give our concrete model set up under A_4 modular symmetry, and formulate mass matrices of Majorana heavy neutrinos, inert scalar bosons, and active neutrinos. Then, we explain how to compare the experimental values. In section 3, we show how to realize the resonant leptogenesis in our model. In section 4, we perform the χ^2 numerical analysis, and show our results to satisfy all the experimental constraints. Finally, we conclude and discuss in section 5.

2 Model

In this section, we review a radiative seesaw model in a modular A_4 symmetry. We introduce modular A_4 symmetry and assign $\{1, 1', 1''\}$ for $(\hat{L}_e, \hat{L}_\mu, \hat{L}_\tau)$ and $\{1, 1'', 1'\}$ for $(\hat{e}^c, \hat{\mu}^c, \hat{\tau}^c)$ in order to consider the mass eigenbasis of charged-lepton sector. Their modular weights are assigned to be $\{-2, -2, 0\}$ for each family. Note here that notation \hat{f} for a field f indicates matter chiral superfield including boson and fermion, otherwise f denotes boson or fermion with even R -parity. In addition, we introduce three electrically neutral superfields \hat{N}^c as discussed in introduction. Then, we add $\hat{\eta}_1$ with -3 modular weight whose corresponding scalar field is important to connect the active neutrinos and the Majorana fermions, while $\hat{\eta}_2$ is introduced only to cancel the gauge chiral anomaly and this field does not contribute to the neutrino sector.⁶ The field contents and their assignments are summarized in table 1.

2.1 Majorana mass matrix

At first, we develop our discussion on the mass matrix of Majorana fermion N given in eq. (1.3). At nearby $\tau = i\infty$, (y_1, y_2, y_3) is expanded by p_ϵ and given by $(1 + 12p_\epsilon,$

⁶ \hat{H}_2 is requested by obtaining the SM Higgs mass through μ term. But, we suppose H_2 does not contribute to our main discussion as well.

$-6p_\epsilon^{1/3}, -18p_\epsilon^{2/3}$), where $|p_\epsilon| \equiv |e^{2\pi i\tau}| \ll 1$ and (y_1, y_2, y_3) is given in appendix A. Then, the Majorana mass matrix in eq. (1.3) is rewritten by

$$M_N \approx M_0 \begin{bmatrix} 2(1+12p_\epsilon) & 18p_\epsilon^{2/3} & 6p_\epsilon^{1/3} \\ 18p_\epsilon^{2/3} & -12p_\epsilon^{1/3} & -(1+12p_\epsilon) \\ 6p_\epsilon^{1/3} & -(1+12p_\epsilon) & -36p_\epsilon^{2/3} \end{bmatrix}. \quad (2.1)$$

It is diagonalized by a unitary matrix U_N as $D \equiv U_N^* M_N U_N^\dagger$, and their mass eigenstates are defined by ψ , where $N = U_N^\dagger \psi$. Therefore, $|D|^2 = U_N M_N^\dagger M_N U_N^\dagger$. Approximately U_N and $|D|$ are given by the following forms:

$$U_N \approx \begin{bmatrix} -3\sqrt{2}p_\epsilon^{1/3}(1-6p_\epsilon^{1/3}) - \frac{1}{\sqrt{2}}(1-3\epsilon^{1/3} + \frac{9}{2}p_\epsilon^{2/3}) & \frac{1}{\sqrt{2}}(1+3\epsilon^{1/3} - \frac{63}{2}p_\epsilon^{2/3}) \\ -\sqrt{2}p_\epsilon^{1/3}(1-2p_\epsilon^{1/3}) & \frac{1}{\sqrt{2}}(1+3\epsilon^{1/3} - \frac{35}{2}p_\epsilon^{2/3}) & \frac{1}{\sqrt{2}}(1-3\epsilon^{1/3} + \frac{13}{2}p_\epsilon^{2/3}) \\ 1-10p_\epsilon^{1/3} & -2p_\epsilon^{1/3}(1-14p_\epsilon^{1/3}) & 2p_\epsilon^{1/3}(2-7p_\epsilon^{1/3}) \end{bmatrix}^* + \mathcal{O}(p_\epsilon), \quad (2.2)$$

$$|D| \approx M_0 \text{diag.} [1-6p_\epsilon^{1/3}-18p_\epsilon^{2/3}, 1+6p_\epsilon^{1/3}+42p_\epsilon^{2/3}, 2+24p_\epsilon^{2/3}] + \mathcal{O}(p_\epsilon). \quad (2.3)$$

Thus, one can straightforwardly find that $|D| = M_0 \text{diag.}[1, 1, 2]$ in the limit of $\tau \rightarrow i\infty$.

2.2 Inert scalar boson mass matrices

Inert scalar boson components of $\hat{\eta}_{1,2}$ and $\hat{\chi}$ contribute to the neutrino mass matrix. The relevant Lagrangian among these bosons is given via soft SUSY-breaking terms as follows:

$$-\mathcal{L}_{\text{soft}} = m_A H_2 \eta_1 \chi + m_B^2 \chi^2 + m_{\eta_1}^2 |\eta_1|^2 + m_\chi^2 |\chi|^2 + m_{H_1}^2 |H_1|^2 + m_{H_2}^2 |H_2|^2 + m_{\eta_2}^2 |\eta_2|^2 + \mu_{BH}^2 H_1 H_2 + \mu_{B\eta}^2 \eta_1 \eta_2 + m'_A H_1 \eta_2 \chi + \text{h.c.}, \quad (2.4)$$

where the terms in the first line of r.h.s. directly contribute to the neutrino mass matrix and some of mass parameters include modular forms. When the neutral components are written in terms of real and imaginary part as $\chi = (\chi_R + i\chi_I)/\sqrt{2}$ and $\eta_1 = (\eta_1^+, (\eta_{R1} + i\eta_{I1})/\sqrt{2})^T$, the mass squared matrices in basis of $(\eta_1, \chi)_{R,I}$ are given by

$$m_R^2 = \begin{bmatrix} m_{\eta_1}^2 & \frac{v_2 m_A}{\sqrt{2}} \\ \frac{v_2 m_A}{\sqrt{2}} & m_\chi^2 + m_B^2 \end{bmatrix}, \quad m_I^2 = \begin{bmatrix} m_{\eta_1}^2 & -\frac{v_2 m_A}{\sqrt{2}} \\ -\frac{v_2 m_A}{\sqrt{2}} & m_\chi^2 - m_B^2 \end{bmatrix}, \quad (2.5)$$

these are diagonalized by $D_{R,I}^2 = O_{R,I} M_{R,I}^2 O_{R,I}^T$, where $O_{R,I}$ is an orthogonal matrix;

$$\begin{bmatrix} \eta_1 \\ \chi \end{bmatrix}_{R,I} = \begin{bmatrix} c_{R,I} & s_{R,I} \\ -s_{R,I} & c_{R,I} \end{bmatrix} \begin{bmatrix} \varphi_1 \\ \varphi_2 \end{bmatrix}_{R,I}, \quad O_{R,I} = \begin{bmatrix} c_{R,I} & s_{R,I} \\ -s_{R,I} & c_{R,I} \end{bmatrix}. \quad (2.6)$$

Here $\varphi_{1R,2R,1I,2I}$ are mass eigenvectors, $s_{R,I}$, $c_{R,I}$ are respectively short-hand notations for $\sin \theta_{R,I}$, $\cos \theta_{R,I}$ which are given by a function of mass parameters in eq. (2.5).

2.3 Neutrino sector

Now we can discuss the neutrino sector estimating neutrino mass at one-loop level. Our valid renormalizable Lagrangian in terms of mass eigenstates of heavier Majorana fermions and inert scalar bosons, coming from superpotential, is given by

$$-\mathcal{L}^\nu = \frac{1}{\sqrt{2}} \bar{\psi}_i (U_N)_{ia} y_{\eta ab} \nu_b (c_R \varphi_{1R} + s_R \varphi_{2R}) + \frac{i}{\sqrt{2}} \bar{\psi}_i (U_N)_{ia} y_{\eta ab} \nu_b (c_I \varphi_{1I} + s_I \varphi_{2I}) + \text{h.c.}, \quad (2.7)$$

$$y_\eta = \begin{bmatrix} a_\eta & 0 & 0 \\ 0 & b_\eta & 0 \\ 0 & 0 & c_\eta \end{bmatrix} \begin{bmatrix} y_1^{(6)} + \epsilon_e y_1'^{(6)} & y_3^{(6)} + \epsilon_e y_3'^{(6)} & y_2^{(6)} + \epsilon_e y_2'^{(6)} \\ y_3^{(6)} + \epsilon_\mu y_3'^{(6)} & y_2^{(6)} + \epsilon_\mu y_2'^{(6)} & y_1^{(6)} + \epsilon_\mu y_1'^{(6)} \\ y_2^{(4)} & y_1^{(4)} & y_3^{(4)} \end{bmatrix}, \quad (2.8)$$

where a_η , b_η , c_η are real without loss of generality after phase redefinition, while $\epsilon_{e,\mu}$ are complex values which would also be sources of CP asymmetry in addition to τ .⁷ Explicit forms of $(y_1^{(4)}, y_2^{(4)}, y_3^{(4)})$, $(y_1^{(6)}, y_2^{(6)}, y_3^{(6)})$, and $(y_1'^{(6)}, y_2'^{(6)}, y_3'^{(6)})$ are given in appendix A. Then, the neutrino mass matrix is given as follows:

$$(m_\nu)_{ab} = -\frac{1}{2(4\pi)^2} (y_\eta)_{a\beta}^T (U_N^T)_{\beta i} D_i (U_N)_{i\alpha} (y_\eta)_{\alpha b} \\ \times \left[c_R^2 F(m_{\varphi_{1R}}, D_i) - c_I^2 F(m_{\varphi_{1I}}, D_i) + s_R^2 F(m_{\varphi_{2R}}, D_i) - s_I^2 F(m_{\varphi_{2I}}, D_i) \right], \quad (2.9)$$

where

$$F(m_a, m_b) = \frac{\ln\left(\frac{m_a^2}{m_b^2}\right)}{\frac{m_a^2}{m_b^2} - 1} - 1. \quad (2.10)$$

The neutrino mass matrix m_ν is then diagonalized by an unitary matrix U_{PMNS} ; $U_{\text{PMNS}}^T m_\nu U_{\text{PMNS}} \equiv \text{diag}(m_1, m_2, m_3)$. We write two mass squared differences measured by the experiments,

$$\Delta m_{\text{sol}}^2 = m_2^2 - m_1^2, \quad (2.11)$$

$$\text{(NH)} : \Delta m_{\text{atm}}^2 = m_3^2 - m_1^2, \quad \text{(IH)} : \Delta m_{\text{atm}}^2 = m_2^2 - m_3^2, \quad (2.12)$$

where Δm_{sol}^2 is solar mass squared difference and Δm_{atm}^2 is atmospheric neutrino mass squared difference whose form depends on whether neutrino mass ordering is normal hierarchy (NH) or inverted hierarchy (IH). U_{PMNS} is parametrized by three mixing angle θ_{ij} ($i, j = 1, 2, 3; i < j$), one CP violating Dirac phase δ_{CP} , and two Majorana phases $\{\alpha_{21}, \alpha_{32}\}$ as follows:

$$U_{\text{PMNS}} = \begin{pmatrix} c_{12}c_{13} & s_{12}c_{13} & s_{13}e^{-i\delta_{CP}} \\ -s_{12}c_{23} - c_{12}s_{23}s_{13}e^{i\delta_{CP}} & c_{12}c_{23} - s_{12}s_{23}s_{13}e^{i\delta_{CP}} & s_{23}c_{13} \\ s_{12}s_{23} - c_{12}c_{23}s_{13}e^{i\delta_{CP}} & -c_{12}s_{23} - s_{12}c_{23}s_{13}e^{i\delta_{CP}} & c_{23}c_{13} \end{pmatrix} \begin{pmatrix} 1 & 0 & 0 \\ 0 & e^{i\frac{\alpha_{21}}{2}} & 0 \\ 0 & 0 & e^{i\frac{\alpha_{31}}{2}} \end{pmatrix}, \quad (2.13)$$

⁷In our model building, we start at a simplest model that has Yukawas with modular weight 2. However we could not find parameter space that can accommodate observed data due to smallness of number of free parameters. Then, we have reached this form of eq. (2.8) to satisfy the neutrino oscillation data and BAU in the framework of resonant leptogenesis, simultaneously. Therefore, it is one of the simplest assignments.

where c_{ij} and s_{ij} stands for $\cos \theta_{ij}$ and $\sin \theta_{ij}$ respectively. Then, each mixing angle is given in terms of the component of U_{PMNS} as follows:

$$\sin^2 \theta_{13} = |(U_{\text{PMNS}})_{13}|^2, \quad \sin^2 \theta_{23} = \frac{|(U_{\text{PMNS}})_{23}|^2}{1 - |(U_{\text{PMNS}})_{13}|^2}, \quad \sin^2 \theta_{12} = \frac{|(U_{\text{PMNS}})_{12}|^2}{1 - |(U_{\text{PMNS}})_{13}|^2}. \quad (2.14)$$

Also, we compute the Jarlskog invariant, δ_{CP} derived from PMNS matrix elements $U_{\alpha i}$:

$$J_{CP} = \text{Im}[U_{e1}U_{\mu 2}U_{e2}^*U_{\mu 1}^*] = s_{23}c_{23}s_{12}c_{12}s_{13}c_{13}^2 \sin \delta_{CP}, \quad (2.15)$$

and the Majorana phases are also estimated in terms of other invariants I_1 and I_2 :

$$I_1 = \text{Im}[U_{e1}^*U_{e2}] = c_{12}s_{12}c_{13}^2 \sin \left(\frac{\alpha_{21}}{2} \right), \quad I_2 = \text{Im}[U_{e1}^*U_{e3}] = c_{12}s_{13}c_{13} \sin \left(\frac{\alpha_{31}}{2} - \delta_{CP} \right). \quad (2.16)$$

Additionally, the effective mass for the neutrinoless double beta decay is given by

$$\langle m_{ee} \rangle = |m_1 \cos^2 \theta_{12} \cos^2 \theta_{13} + m_2 \sin^2 \theta_{12} \cos^2 \theta_{13} e^{i\alpha_{21}} + m_3 \sin^2 \theta_{13} e^{i(\alpha_{31} - 2\delta_{CP})}|, \quad (2.17)$$

where its observed value could be measured by KamLAND-Zen in future [83]. We will adopt the neutrino experimental data in NuFit5.0 [84] in order to perform the numerical χ^2 analysis.

3 Resonant leptogenesis

Now we consider non-thermal leptogenesis where population of the lightest sterile neutrino increases as the temperature decreases, so-called freeze-in production. The generation of the lepton asymmetry is non-equilibrium decay process of the lightest neutrino ψ_1 . The dominant contribution to the CP asymmetry is arisen from the interference between tree and one-loop diagrams for decays of ψ_1 via Yukawa coupling y_η . In general, there are two one-loop decay modes; vertex correction diagram and self-energy correction, but the self energy correction is dominant in our case since ψ_1 and ψ_2 have degenerate mass. Hence, the main source of CP asymmetry ϵ_1 is approximately given as follows:

$$\epsilon_1 \approx \frac{\text{Im}(h^\dagger h)_{12}^2}{(h^\dagger h)_{11}^2 (h^\dagger h)_{22}^2} \frac{(D_1^2 - D_2^2) D_1 \Gamma_2}{(D_1^2 - D_2^2)^2 + D_1^2 \Gamma_{\psi_2}^2}, \quad (3.1)$$

$$\Gamma_{\psi_2} = \frac{|h_{2i}|^2}{4\pi} D_2 \left(1 - \frac{m_{\eta_1}^2}{D_2^2} \right)^2, \quad (3.2)$$

where $h \equiv U_N y_\eta$, and we expect $m_{\eta_1} \approx m_{\varphi_{1R}} \approx m_{\varphi_{1I}}$. Then, we obtain the lepton asymmetry by solving the approximated Boltzmann equations for ψ_1 and lepton number densities as follows:

$$\frac{dY_{\psi_1}}{dz} \approx -\frac{z}{sH(D_1)} \left(\frac{Y_{\psi_1}}{Y_{\psi_1}^{eq}} - 1 \right) \gamma_D^{\psi_1}, \quad (3.3)$$

$$\frac{dY_L}{dz} \approx \frac{z}{sH(D_1)} \left(\frac{Y_{\psi_1}}{Y_{\psi_1}^{eq}} - 1 \right) \epsilon_1 \gamma_D^{\psi_1}, \quad (3.4)$$

$$\gamma_D^{\psi_1} = \sum_{i=1}^3 \frac{|h_{1i}|^2}{4\pi^3} D_1^4 \left(1 - \frac{m_{\eta_1}^2}{D_1^2} \right)^2 \frac{K_1(z)}{z}, \quad (3.5)$$

where $z \equiv D_1/T$, T being temperature, $H(D_1) = 1.66g_*^{1/2}D_1^2/M_{pl}$, $g_* \approx 100$ is the number of relativistic degrees of freedom, and Plank mass $M_{pl} \approx 1.2 \times 10^{19}$ GeV. We denote the entropy density as $Y_{\psi_1} \equiv n_{\psi_1}/s$ and $Y_L \equiv (n_L - n_{\bar{L}})/s$, $s = 2\pi^2g_*T^3/45$. Furthermore, $Y_{\psi_1}^{eq}$ is given by $45z^2K_2(z)/(2\pi^4g_*)$, $K_{1(2)}(z)$, where $K_{1(2)}(z)$ is the modified Bessel function of the first(second) kind. Once the lepton asymmetry Y_L is generated, it is converted by $B + L$ violating spharelon transitions [85, 86]. Then, the conversion rate is straightforwardly derived by the chemical equilibrium conditions and it is found as

$$Y_B = -\frac{8}{23}Y_L(z_{EW}), \tag{3.6}$$

where z_{EW} corresponds to the spharelon decoupling temperature and we set to be $T_{EW} = 100$ GeV. Here, we should mention scattering processes that should be included in the above Boltzmann equations in general, since these processes also change the number of lepton as well as ψ . The lepton number is changed by the processes of $\ell\ell \rightarrow \eta\eta$ and $\eta\ell \rightarrow \eta^\dagger\bar{\ell}$, and the change of ψ_1 number is caused by $\psi_1\psi_1 \rightarrow \ell\bar{\ell}$ and $\psi_1\psi_1 \rightarrow \eta\eta^\dagger$ [79]. Even though there exist resonant enhancement, the wash out processes from these scattering processes could be dominant depending on the parameter region. In order to suppress these processes enough, we should work on, e.g., $D_1 \lesssim 2.5$ TeV when $|h| \approx 10^{-4}$.⁸ Otherwise, we have to include the scattering processes. In our numerical analysis, we compute the simplified Boltzmann equations by carefully checking whether the washout processes can be neglected or not for our allowed parameter sets from neutrino data fitting. In addition, the number density of N_1 is generated by freeze-in mechanism and it becomes the same order as that of thermal equilibrium for temperature higher than electroweak scale.

4 Numerical analysis

In this section, we carry out numerical analysis searching for allowed parameter region satisfying phenomenological constraints. *Note first that we find there is no allowed regions simultaneously satisfying the observed neutrino oscillation data and BAU in case of IH. Thus, we focus on the case of NH only.* We show the allowed region with χ^2 analysis in the lepton sector, where we randomly select the values of input parameters within the following ranges,

$$\begin{aligned} |\text{Re}(\tau)| &\in [10^{-3}, 0.5], & \text{Im}(\tau) &\in [2, 10], & \{a_\eta, b_\eta, c_\eta\} &\in [10^{-8}, 10^{-3}], \\ \{|\epsilon_e|, |\epsilon_\mu|\} &\in [10^{-3}, 10^3], & M_0 &\in [10^2, 10^5] \text{ GeV}, & m_{\eta_1} &\in [70, 10^3] \text{ GeV}, \\ m_\chi &\in [1, 10^3] \text{ GeV}, & \{m_A, m_B\} &\in [0.001, 50] \text{ GeV}, & & \end{aligned} \tag{4.1}$$

where we expect the source of CP asymmetry arises from three complex values τ , ϵ_e , ϵ_μ . We also require inert scalar bosons are lighter than ψ_1 so that ψ_1 can decay into scalar boson and lepton to realize leptogenesis. Then, we accumulate the data if five measured neutrino

⁸The order 10^{-4} comes from a prior research in ref. [79]. In this situation, LFVs are suppressed enough to satisfy the current experiments. In fact, the stringent constraint of $\mu \rightarrow e\gamma$ gives 4.2×10^{-13} of the branching ratio, while our maximum value of this process is 10^{-16} at most in our numerical analysis. Thus, we do not mention LFVs furthermore.

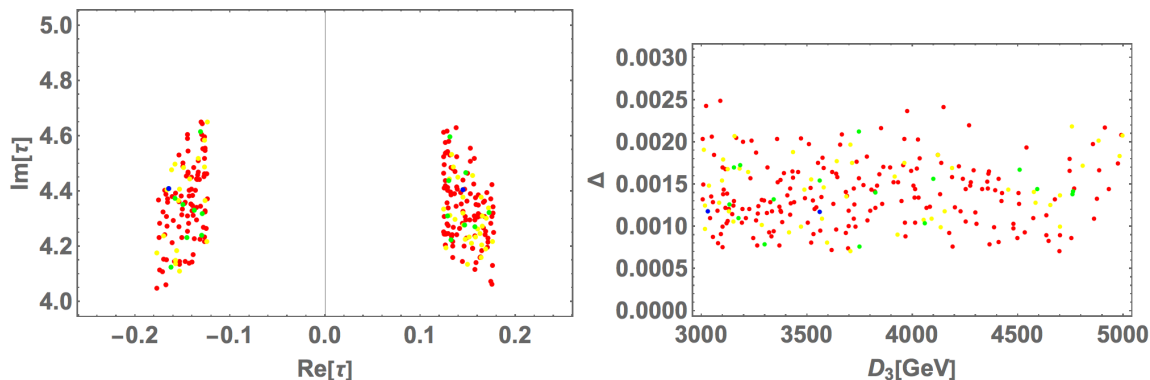


Figure 1. The left plot shows allowed region of τ , while the right one shows the mass degeneracy of D_1 and D_2 that is defined by $\Delta \equiv (D_2 - D_1)/D_2$ in terms of D_3 in GeV unit, where $D_2(\sim D_1) \sim D_3/2$. Each point in blue, green, yellow, and red color represents the allowed region in $\sigma \leq 1$, $1 < \sigma \leq 2$, $2 < \sigma \leq 3$, and $3 < \sigma \leq 5$ interval, respectively.

oscillation data; $(\Delta m_{\text{atm}}^2, \Delta m_{\text{sol}}^2, \sin^2 \theta_{13}, \sin^2 \theta_{23}, \sin^2 \theta_{12})$ [84] and BAU in eq. (1.2) are satisfied at the same time. Notice here that we regard δ_{CP} as a predicted value due to large ambiguity of experimental result in 3σ interval.

The left plot of figure 1 shows allowed region of τ , while the right one shows the mass degeneracy of D_1 and D_2 that is defined by $\Delta \equiv (D_2 - D_1)/D_2$ in terms of D_3 in GeV unit, where $D_2(\sim D_1) \sim D_3/2$. Each point in blue, green, yellow, and red color represents the allowed region in $\sigma \leq 1$, $1 < \sigma \leq 2$, $2 < \sigma \leq 3$, and $3 < \sigma \leq 5$ interval, respectively. These figures suggest that $0.12 \lesssim \text{Re}|\tau| \lesssim 0.18$ and $4.05 \lesssim \text{Im}[\tau] \lesssim 4.65$, $7 \times 10^{-4} \lesssim \Delta \lesssim 2.5 \times 10^{-3}$, and $3000 \text{ GeV} \lesssim D_3 \lesssim 5000 \text{ GeV}$. Note here that the smaller Δ directly corresponds to the larger imaginary part of τ , while the $\text{Re}[\tau]$ plays a role in generating one of the CP sources together with $\epsilon_{e,\mu}$. We thus find sizable $\text{Re}[\tau]$ value is required in our allowed region and it suggests that *the main source of CP asymmetry would arise from τ* .⁹

In order to investigate the main source of CP asymmetry, we demonstrate the plots of arguments of $\epsilon_{e,\mu}$ in terms of $\text{Re}[\tau]$ in figure 2, where the color legends are the same as the one in figure 1. Remarkably, argument of ϵ_μ is almost zero while the one of ϵ_e is slightly deviated from zero. It comes from the resonant leptogenesis and neutrino oscillation. In order to achieve the resonant leptogenesis, we need $(y_1, y_2, y_3) \sim (1, 0, 0)$. It implies that $(y_1^{(6)}, y_2^{(6)}, y_3^{(6)}) \sim (1, 0, 0)$ and $(y_1'^{(6)}, y_2'^{(6)}, y_3'^{(6)}) \sim (0, 0, 0)$, leading y_η to

$$y_\eta \sim \begin{bmatrix} 1 & 0 & 0 \\ 0 & 0 & 1 \\ 0 & 1 & 0 \end{bmatrix}. \quad (4.2)$$

On the other hand, $y_{\eta_{12,13}} \ll y_{\eta_{21,32}}$ are required in order to obtain the observable neutrino oscillation data. In order to compensate the tiny components of $Y_3^{(6)}, Y_{3'}^{(6)}$, rather large value of $\text{Re}[\epsilon_\mu]$ is needed. Thus, the argument of ϵ_μ is relatively tiny. Since both the

⁹In general, ϵ_μ has to be complex parameter after phase redefinition of fields. But, as an experimental point of view, real ϵ_μ is allowed from our numerical result and we can assume this parameter to be real.

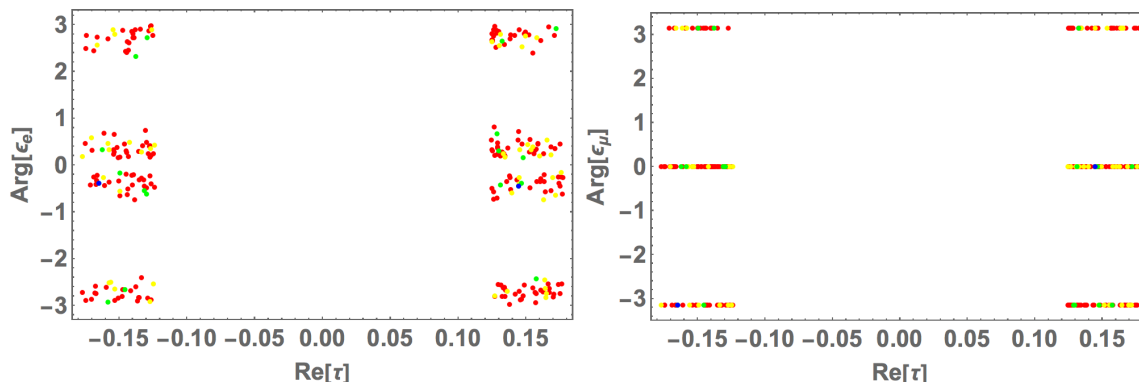


Figure 2. The left (right) plot shows allowed region of $\text{Arg}[\epsilon_{e(\mu)}]$ in terms of $\text{Re}[\tau]$, where the color legends are the same as the one in figure 1.

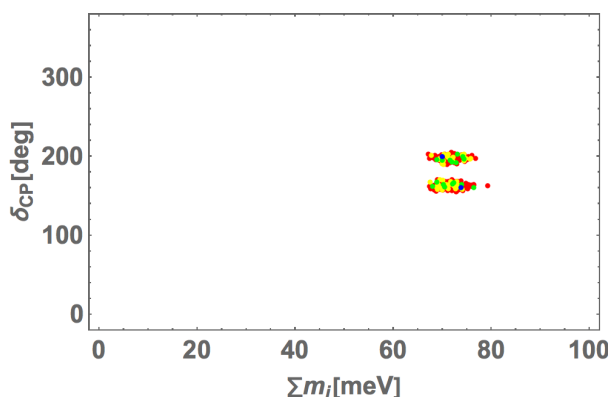


Figure 3. Allowed region of δ_{CP} in terms of $\sum m_i$, where the color legends are the same as the one in figure 1.

arguments of $\epsilon_{e,\mu}$ are localized at nearby 0 and π , *the main origin of CP asymmetry indeed originates from τ .*

The figure 3 shows the allowed region of δ_{CP} in terms of $\sum m_i$, where the color legends are the same as the one in figure 1. We find two small localized regions of $150^\circ \lesssim \delta_{\text{CP}} \lesssim 170^\circ$ and $180^\circ \lesssim \delta_{\text{CP}} \lesssim 200^\circ$ with $65 \text{ meV} \lesssim \sum m_i \lesssim 80 \text{ meV}$, where the up island corresponds to the region of $\text{Re}[\tau] < 0$ while the down one corresponds to the region of $\text{Re}[\tau] > 0$. *Our result would favor the best fit value of $\delta_{\text{CP}} = 195^\circ$.*

The figure 4 shows Majorana phases α_{21} and α_{31} , where the color legends are the same as the one in figure 1. We have two localized islands of $10^\circ \lesssim \alpha_{21} \lesssim 30^\circ$, $55^\circ \lesssim \alpha_{31} \lesssim 80^\circ$, and $330^\circ \lesssim \alpha_{21} \lesssim 360^\circ$, $280^\circ \lesssim \alpha_{31} \lesssim 310^\circ$, where the up-right island corresponds to the region of $\text{Re}[\tau] < 0$ while the down-left one corresponds to the region of $\text{Re}[\tau] > 0$.

The figure 5 shows $\langle m_{ee} \rangle$ in terms of the lightest neutrino mass m_1 meV, where the color legends are the same as the one in figure 1. We obtain $7 \text{ meV} \lesssim \langle m_{ee} \rangle \lesssim 12 \text{ meV}$ and $6 \text{ meV} \lesssim m_1 \lesssim 13 \text{ meV}$.

We show the baryon asymmetry Y_B in terms of the CP asymmetry source ϵ_1 in figure 6, where the color legends are the same as the one in figure 1 and the Y_B is taken within the

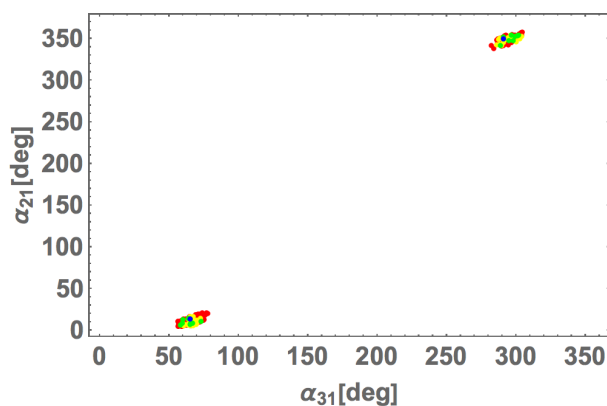


Figure 4. Allowed region of Majorana phases α_{21} and α_{31} , where the color legends are the same as the one in figure 1.

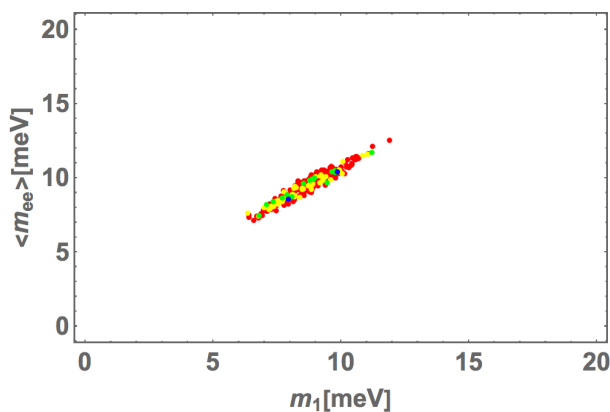


Figure 5. Allowed region of $\langle m_{ee} \rangle$ in terms of the lightest neutrino mass m_1 meV, where the color legends are the same as the one in figure 1.

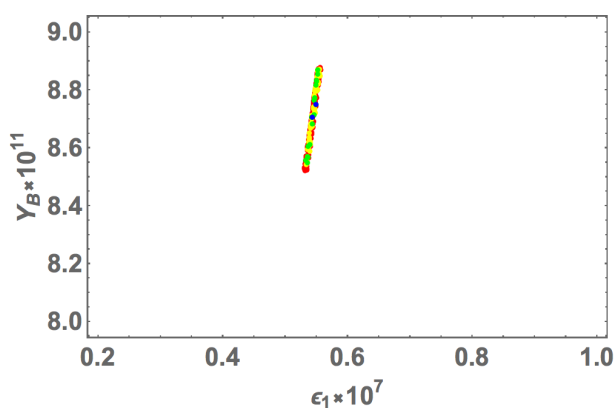


Figure 6. Allowed region of the baryon asymmetry Y_B in terms of the CP asymmetry source ϵ_1 , where the color legends are the same as the one in figure 1 and the Y_B is taken within the observed range in eq. (1.2).

	NH
τ	$-0.165 + 4.41i$
$[a_\eta, b_\eta, c_\eta] \times 10^5$	$[-4.94, -8.42, 6.71]$
$[M_0, M_{\eta_1}, m_\chi]/\text{GeV}$	$[1780, 199, 70.9]$
$[(v_2 m_A/\sqrt{2})^{1/2}, m_B]/\text{GeV}$	$[45.1, 0.0324]$
$[\epsilon_e, \epsilon_\mu]$	$[24.0 - 9.80i, -761 - 0.00522i]$
Δm_{atm}^2	$2.47 \times 10^{-3} \text{eV}^2$
Δm_{sol}^2	$7.37 \times 10^{-5} \text{eV}^2$
$\sin \theta_{12}$	0.544
$\sin \theta_{23}$	0.743
$\sin \theta_{13}$	0.151
$[\delta_{CP}^\ell, \alpha_{21}, \alpha_{31}]$	$[200^\circ, 349^\circ, 291^\circ]$
$\sum m_i$	70 meV
$\langle m_{ee} \rangle$	8.58 meV
ϵ_1	5.43×10^{-8}
Y_B	8.71×10^{-11}
$\sqrt{\Delta\chi^2}$	1.90

Table 2. Numerical benchmark point of our input parameters and observables at nearby the fixed point $\tau = i \times \infty$ in NH. Here, we take BP so that δ_{CP} is closest to the BF value of 195° within $\sqrt{\Delta\chi^2} \leq 1$.

observed range in eq. (1.2). Here, ϵ_1 is about 5×10^{-8} that is favored by the prior analysis in ref. [79]. Finally, we show a benchmark point for NH in table 2 that provide minimum $\sqrt{\chi^2}$ in our numerical analysis.

5 Conclusion and discussion

We explore a modular A_4 invariant radiative seesaw model. In this model, we can generate the measured baryon asymmetry via resonant leptogenesis as well as the observed neutrino oscillation data. Larger $\text{Im}[\tau]$ leads to the more degenerate Majorana masses. This degenerate masses are preferred by the resonant leptogenesis since larger $\text{Im}[\tau]$ can enhance the CP asymmetry and avoid the washout processes even though keeping the small Yukawa couplings. While the nonzero $\text{Re}[\tau]$ provides the source of CP asymmetry in addition to free complex parameters. In our case, especially, $\text{Re}[\tau]$ is main source of the CP asymmetry by our χ^2 numerical analysis that would be interesting result in this scenario. Since the constraint of BAU in eq. (1.2) is very strict, we have obtained narrow allowed region as we

have discussed in the numerical analysis. Below, we have highlightend several remarks on the neutrino sector,

1. We have obtained two small localized regions of $150^\circ \lesssim \delta_{\text{CP}} \lesssim 170^\circ$ and $180^\circ \lesssim \delta_{\text{CP}} \lesssim 200^\circ$ with $65 \text{ meV} \lesssim \sum m_i \lesssim 80 \text{ meV}$, where $180^\circ \lesssim \delta_{\text{CP}} \lesssim 200^\circ$ corresponds to the region of $\text{Re}[\tau] < 0$ while $150^\circ \lesssim \delta_{\text{CP}} \lesssim 170^\circ$ corresponds to the region of $\text{Re}[\tau] > 0$. *Our result would favor the best fit value of $\delta_{\text{CP}} = 195^\circ$.*
2. We have found two localized islands of $10^\circ \lesssim \alpha_{21} \lesssim 30^\circ$, $55^\circ \lesssim \alpha_{31} \lesssim 80^\circ$, and $330^\circ \lesssim \alpha_{21} \lesssim 360^\circ$, $280^\circ \lesssim \alpha_{31} \lesssim 310^\circ$, where $330^\circ \lesssim \alpha_{21} \lesssim 360^\circ$, $280^\circ \lesssim \alpha_{31} \lesssim 310^\circ$ corresponds to the region of $\text{Re}[\tau] < 0$ while $10^\circ \lesssim \alpha_{21} \lesssim 30^\circ$, $55^\circ \lesssim \alpha_{31} \lesssim 80^\circ$ one corresponds to the region of $\text{Re}[\tau] > 0$.
3. We have gotten $7 \text{ meV} \lesssim \langle m_{ee} \rangle \lesssim 12 \text{ meV}$ and $6 \text{ meV} \lesssim m_1 \lesssim 13 \text{ meV}$.

Furthermore, our heavy neutrino masses and inert scalar bosons are order of several hundred GeV to $\mathcal{O}(\text{TeV})$ scale. We thus expect that our model can be tested at collider experiments such as the LHC. For example, inert scalar bosons from doublet can be produced via electroweak interactions. Detailed collider analysis is beyond the scope of this paper and it will be done in future work.

Acknowledgments

This work is in part supported by KIAS Individual Grants, Grant No. PG074202 (JK) and Grant No. PG076202 (DWK) at Korea Institute for Advanced Study. This research was supported by an appointment to the JRG Program at the APCTP through the Science and Technology Promotion Fund and Lottery Fund of the Korean Government. This was also supported by the Korean Local Governments — Gyeongsangbuk-do Province and Pohang City (H.O.). H.O. is sincerely grateful for the KIAS member, and log cabin at POSTECH to provide nice space to come up with this project. The work was also supported by the Fundamental Research Funds for the Central Universities (T.N.).

A Formulas in modular A_4 framework

Here we summarize some formulas of A_4 modular symmetry framework. Modular forms are holomorphic functions of modulus τ , $f(\tau)$, which are transformed by

$$\tau \longrightarrow \gamma\tau = \frac{a\tau + b}{c\tau + d}, \quad \text{where } a, b, c, d \in \mathbb{Z} \text{ and } ad - bc = 1, \quad \text{Im}[\tau] > 0, \quad (\text{A.1})$$

$$f(\gamma\tau) = (c\tau + d)^k f(\tau), \quad \gamma \in \Gamma(N), \quad (\text{A.2})$$

where k is the so-called as the modular weight.

A superfield $\phi^{(I)}$ is transformed under the modular transformation as

$$\phi^{(I)} \longrightarrow (c\tau + d)^{-k_I} \rho^{(I)}(\gamma) \phi^{(I)}, \quad (\text{A.3})$$

where $-k_I$ is the modular weight and $\rho^{(I)}(\gamma)$ represents an unitary representation matrix corresponding to A_4 transformation. Thus superpotential is invariant if sum of modular weight from fields and modular form in corresponding term is zero (also it should be invariant under A_4 and gauge symmetry).

The basis of modular forms is weight 2, $Y_3^{(2)} = (y_1, y_2, y_3)$, transforming as a triplet of A_4 that is written in terms of the Dedekind eta-function $\eta(\tau)$ and its derivative [12]:

$$\begin{aligned} y_1(\tau) &= \frac{i}{2\pi} \left(\frac{\eta'(\tau/3)}{\eta(\tau/3)} + \frac{\eta'((\tau+1)/3)}{\eta((\tau+1)/3)} + \frac{\eta'((\tau+2)/3)}{\eta((\tau+2)/3)} - \frac{27\eta'(3\tau)}{\eta(3\tau)} \right), \\ y_2(\tau) &= \frac{-i}{\pi} \left(\frac{\eta'(\tau/3)}{\eta(\tau/3)} + \omega^2 \frac{\eta'((\tau+1)/3)}{\eta((\tau+1)/3)} + \omega \frac{\eta'((\tau+2)/3)}{\eta((\tau+2)/3)} \right), \\ y_3(\tau) &= \frac{-i}{\pi} \left(\frac{\eta'(\tau/3)}{\eta(\tau/3)} + \omega \frac{\eta'((\tau+1)/3)}{\eta((\tau+1)/3)} + \omega^2 \frac{\eta'((\tau+2)/3)}{\eta((\tau+2)/3)} \right), \\ \eta(\tau) &= q^{1/24} \prod_{n=1}^{\infty} (1 - q^n), \quad q = e^{2\pi i \tau}, \quad \omega = e^{2\pi i/3}. \end{aligned} \tag{A.4}$$

Modular forms with higher weight can be obtained from $y_{1,2,3}(\tau)$ through the A_4 multiplication rules as shown the last part. Thus, some A_4 triplet modular forms used in our analysis are derived as follows:

$$Y_3^{(4)} \equiv (y_1^{(4)}, y_2^{(4)}, y_3^{(4)}) = (y_1^2 - y_2 y_3, y_3^2 - y_1 y_2, y_2^2 - y_1 y_3), \tag{A.5}$$

$$Y_3^{(6)} \equiv (y_1^{(6)}, y_2^{(6)}, y_3^{(6)}) = (y_1^3 + 2y_1 y_2 y_3, y_1^2 y_2 + 2y_2^2 y_3, y_1^2 y_3 + 2y_3^2 y_2), \tag{A.6}$$

$$Y_{3'}^{(6)} \equiv (y_1'^{(6)}, y_2'^{(6)}, y_3'^{(6)}) = (y_3^3 + 2y_1 y_2 y_3, y_3^2 y_1 + 2y_1^2 y_2, y_3^2 y_2 + 2y_2^2 y_1). \tag{A.7}$$

A_4 multiplication rules are given by

$$\begin{aligned} \begin{pmatrix} a_1 \\ a_2 \\ a_3 \end{pmatrix}_{\mathbf{3}} \otimes \begin{pmatrix} b_1 \\ b_2 \\ b_3 \end{pmatrix}_{\mathbf{3}'} &= (a_1 b_1 + a_2 b_3 + a_3 b_2)_{\mathbf{1}} \oplus (a_3 b_3 + a_1 b_2 + a_2 b_1)_{\mathbf{1}'} \\ &\quad \oplus (a_2 b_2 + a_1 b_3 + a_3 b_1)_{\mathbf{1}''} \\ &\quad \oplus \frac{1}{3} \begin{pmatrix} 2a_1 b_1 - a_2 b_3 - a_3 b_2 \\ 2a_3 b_3 - a_1 b_2 - a_2 b_1 \\ 2a_2 b_2 - a_1 b_3 - a_3 b_1 \end{pmatrix}_{\mathbf{3}} \oplus \frac{1}{2} \begin{pmatrix} a_2 b_3 - a_3 b_2 \\ a_1 b_2 - a_2 b_1 \\ a_3 b_1 - a_1 b_3 \end{pmatrix}_{\mathbf{3}'}, \\ a_{1'} \otimes \begin{pmatrix} b_1 \\ b_2 \\ b_3 \end{pmatrix}_{\mathbf{3}} &= a \begin{pmatrix} b_3 \\ b_1 \\ b_2 \end{pmatrix}_{\mathbf{3}}, \quad a_{1''} \otimes \begin{pmatrix} b_1 \\ b_2 \\ b_3 \end{pmatrix}_{\mathbf{3}} = a \begin{pmatrix} b_2 \\ b_3 \\ b_1 \end{pmatrix}_{\mathbf{3}}, \\ \mathbf{1} \otimes \mathbf{1} &= \mathbf{1}, \quad \mathbf{1}' \otimes \mathbf{1}' = \mathbf{1}'', \quad \mathbf{1}'' \otimes \mathbf{1}'' = \mathbf{1}', \quad \mathbf{1}' \otimes \mathbf{1}'' = \mathbf{1}. \end{aligned} \tag{A.8}$$

Open Access. This article is distributed under the terms of the Creative Commons Attribution License ([CC-BY 4.0](https://creativecommons.org/licenses/by/4.0/)), which permits any use, distribution and reproduction in any medium, provided the original author(s) and source are credited. SCOAP³ supports the goals of the International Year of Basic Sciences for Sustainable Development.

References

- [1] PLANCK collaboration, *Planck 2018 results. VI. Cosmological parameters*, *Astron. Astrophys.* **641** (2020) A6 [*Erratum ibid.* **652** (2021) C4] [[arXiv:1807.06209](#)] [[INSPIRE](#)].
- [2] A.G. Cohen, D.B. Kaplan and A.E. Nelson, *Progress in electroweak baryogenesis*, *Ann. Rev. Nucl. Part. Sci.* **43** (1993) 27 [[hep-ph/9302210](#)] [[INSPIRE](#)].
- [3] K.-Y. Choi, S.K. Kang and J. Kim, *Non-thermal WIMP baryogenesis*, *Phys. Lett. B* **782** (2018) 657 [[arXiv:1803.00820](#)] [[INSPIRE](#)].
- [4] M. Fukugita and T. Yanagida, *Baryogenesis Without Grand Unification*, *Phys. Lett. B* **174** (1986) 45 [[INSPIRE](#)].
- [5] T. Yanagida, *Horizontal gauge symmetry and masses of neutrinos*, *Conf. Proc. C* **7902131** (1979) 95 [[INSPIRE](#)].
- [6] T. Yanagida, *Horizontal Symmetry and Mass of the Top Quark*, *Phys. Rev. D* **20** (1979) 2986 [[INSPIRE](#)].
- [7] P. Minkowski, $\mu \rightarrow e\gamma$ at a Rate of One Out of 10^9 Muon Decays?, *Phys. Lett. B* **67** (1977) 421 [[INSPIRE](#)].
- [8] R.N. Mohapatra and G. Senjanović, *Neutrino Mass and Spontaneous Parity Nonconservation*, *Phys. Rev. Lett.* **44** (1980) 912 [[INSPIRE](#)].
- [9] A. Pilaftsis and T.E.J. Underwood, *Resonant leptogenesis*, *Nucl. Phys. B* **692** (2004) 303 [[hep-ph/0309342](#)] [[INSPIRE](#)].
- [10] A. Pilaftsis, *CP violation and baryogenesis due to heavy Majorana neutrinos*, *Phys. Rev. D* **56** (1997) 5431 [[hep-ph/9707235](#)] [[INSPIRE](#)].
- [11] M. Flanz, E.A. Paschos, U. Sarkar and J. Weiss, *Baryogenesis through mixing of heavy Majorana neutrinos*, *Phys. Lett. B* **389** (1996) 693 [[hep-ph/9607310](#)] [[INSPIRE](#)].
- [12] F. Feruglio, *Are neutrino masses modular forms?*, in *From My Vast Repertoire...: Guido Altarelli's Legacy*, A. Levy, S. Forte and G. Ridolfi, eds., pp. 227–266 (2019) [[DOI](#)] [[arXiv:1706.08749](#)] [[INSPIRE](#)].
- [13] R. de Adelhart Toorop, F. Feruglio and C. Hagedorn, *Finite Modular Groups and Lepton Mixing*, *Nucl. Phys. B* **858** (2012) 437 [[arXiv:1112.1340](#)] [[INSPIRE](#)].
- [14] J.C. Criado and F. Feruglio, *Modular Invariance Faces Precision Neutrino Data*, *SciPost Phys.* **5** (2018) 042 [[arXiv:1807.01125](#)] [[INSPIRE](#)].
- [15] T. Kobayashi, N. Omoto, Y. Shimizu, K. Takagi, M. Tanimoto and T.H. Tatsuishi, *Modular A_4 invariance and neutrino mixing*, *JHEP* **11** (2018) 196 [[arXiv:1808.03012](#)] [[INSPIRE](#)].
- [16] H. Okada and M. Tanimoto, *CP violation of quarks in A_4 modular invariance*, *Phys. Lett. B* **791** (2019) 54 [[arXiv:1812.09677](#)] [[INSPIRE](#)].
- [17] T. Kobayashi, H. Okada and Y. Orikasa, *Dark matter stability at fixed points in a modular A_4 symmetry*, [arXiv:2111.05674](#) [[INSPIRE](#)].
- [18] T. Nomura and H. Okada, *A modular A_4 symmetric model of dark matter and neutrino*, *Phys. Lett. B* **797** (2019) 134799 [[arXiv:1904.03937](#)] [[INSPIRE](#)].
- [19] H. Okada and M. Tanimoto, *Towards unification of quark and lepton flavors in A_4 modular invariance*, *Eur. Phys. J. C* **81** (2021) 52 [[arXiv:1905.13421](#)] [[INSPIRE](#)].

- [20] F.J. de Anda, S.F. King and E. Perdomo, *SU(5) grand unified theory with A_4 modular symmetry*, *Phys. Rev. D* **101** (2020) 015028 [[arXiv:1812.05620](#)] [[INSPIRE](#)].
- [21] P.P. Novichkov, S.T. Petcov and M. Tanimoto, *Trimaximal Neutrino Mixing from Modular A_4 Invariance with Residual Symmetries*, *Phys. Lett. B* **793** (2019) 247 [[arXiv:1812.11289](#)] [[INSPIRE](#)].
- [22] T. Nomura and H. Okada, *A two loop induced neutrino mass model with modular A_4 symmetry*, *Nucl. Phys. B* **966** (2021) 115372 [[arXiv:1906.03927](#)] [[INSPIRE](#)].
- [23] H. Okada and Y. Orikasa, *A radiative seesaw model in modular A_4 symmetry*, [arXiv:1907.13520](#) [[INSPIRE](#)].
- [24] G.-J. Ding, S.F. King and X.-G. Liu, *Modular A_4 symmetry models of neutrinos and charged leptons*, *JHEP* **09** (2019) 074 [[arXiv:1907.11714](#)] [[INSPIRE](#)].
- [25] T. Kobayashi, Y. Shimizu, K. Takagi, M. Tanimoto and T.H. Tatsuishi, *A_4 lepton flavor model and modulus stabilization from S_4 modular symmetry*, *Phys. Rev. D* **100** (2019) 115045 [*Erratum ibid.* **101** (2020) 039904] [[arXiv:1909.05139](#)] [[INSPIRE](#)].
- [26] T. Asaka, Y. Heo, T.H. Tatsuishi and T. Yoshida, *Modular A_4 invariance and leptogenesis*, *JHEP* **01** (2020) 144 [[arXiv:1909.06520](#)] [[INSPIRE](#)].
- [27] D. Zhang, *A modular A_4 symmetry realization of two-zero textures of the Majorana neutrino mass matrix*, *Nucl. Phys. B* **952** (2020) 114935 [[arXiv:1910.07869](#)] [[INSPIRE](#)].
- [28] G.-J. Ding, S.F. King, X.-G. Liu and J.-N. Lu, *Modular S_4 and A_4 symmetries and their fixed points: new predictive examples of lepton mixing*, *JHEP* **12** (2019) 030 [[arXiv:1910.03460](#)] [[INSPIRE](#)].
- [29] T. Kobayashi, T. Nomura and T. Shimomura, *Type II seesaw models with modular A_4 symmetry*, *Phys. Rev. D* **102** (2020) 035019 [[arXiv:1912.00637](#)] [[INSPIRE](#)].
- [30] T. Nomura, H. Okada and S. Patra, *An inverse seesaw model with A_4 -modular symmetry*, *Nucl. Phys. B* **967** (2021) 115395 [[arXiv:1912.00379](#)] [[INSPIRE](#)].
- [31] X. Wang, *Lepton flavor mixing and CP-violation in the minimal type-(I+II) seesaw model with a modular A_4 symmetry*, *Nucl. Phys. B* **957** (2020) 115105 [[arXiv:1912.13284](#)] [[INSPIRE](#)].
- [32] H. Okada and Y. Shoji, *A radiative seesaw model with three Higgs doublets in modular A_4 symmetry*, *Nucl. Phys. B* **961** (2020) 115216 [[arXiv:2003.13219](#)] [[INSPIRE](#)].
- [33] H. Okada and M. Tanimoto, *Quark and lepton flavors with common modulus τ in A_4 modular symmetry*, [arXiv:2005.00775](#) [[INSPIRE](#)].
- [34] M.K. Behera, S. Singirala, S. Mishra and R. Mohanta, *A modular A_4 symmetric scotogenic model for neutrino mass and dark matter*, *J. Phys. G* **49** (2022) 035002 [[arXiv:2009.01806](#)] [[INSPIRE](#)].
- [35] M.K. Behera, S. Mishra, S. Singirala and R. Mohanta, *Implications of A_4 modular symmetry on neutrino mass, mixing and leptogenesis with linear seesaw*, *Phys. Dark Univ.* **36** (2022) 101027 [[arXiv:2007.00545](#)] [[INSPIRE](#)].
- [36] T. Nomura and H. Okada, *A linear seesaw model with A_4 -modular flavor and local $U(1)_{B-L}$ symmetries*, [arXiv:2007.04801](#) [[INSPIRE](#)].
- [37] T. Nomura and H. Okada, *Modular A_4 symmetric inverse seesaw model with $SU(2)_L$ multiplet fields*, [arXiv:2007.15459](#) [[INSPIRE](#)].

- [38] T. Asaka, Y. Heo and T. Yoshida, *Lepton flavor model with modular A_4 symmetry in large volume limit*, *Phys. Lett. B* **811** (2020) 135956 [[arXiv:2009.12120](#)] [[INSPIRE](#)].
- [39] H. Okada and M. Tanimoto, *Modular invariant flavor model of A_4 and hierarchical structures at nearby fixed points*, *Phys. Rev. D* **103** (2021) 015005 [[arXiv:2009.14242](#)] [[INSPIRE](#)].
- [40] K.I. Nagao and H. Okada, *Lepton sector in modular A_4 and gauged $U(1)_R$ symmetry*, *Nucl. Phys. B* **980** (2022) 115841 [[arXiv:2010.03348](#)] [[INSPIRE](#)].
- [41] H. Okada and M. Tanimoto, *Spontaneous CP-violation by modulus τ in A_4 model of lepton flavors*, *JHEP* **03** (2021) 010 [[arXiv:2012.01688](#)] [[INSPIRE](#)].
- [42] C.-Y. Yao, J.-N. Lu and G.-J. Ding, *Modular Invariant A_4 Models for Quarks and Leptons with Generalized CP Symmetry*, *JHEP* **05** (2021) 102 [[arXiv:2012.13390](#)] [[INSPIRE](#)].
- [43] F. Feruglio, V. Gherardi, A. Romanino and A. Titov, *Modular invariant dynamics and fermion mass hierarchies around $\tau = i$* , *JHEP* **05** (2021) 242 [[arXiv:2101.08718](#)] [[INSPIRE](#)].
- [44] P. Chen, G.-J. Ding and S.F. King, *SU(5) GUTs with A_4 modular symmetry*, *JHEP* **04** (2021) 239 [[arXiv:2101.12724](#)] [[INSPIRE](#)].
- [45] M. Kashav and S. Verma, *Broken scaling neutrino mass matrix and leptogenesis based on A_4 modular invariance*, *JHEP* **09** (2021) 100 [[arXiv:2103.07207](#)] [[INSPIRE](#)].
- [46] H. Okada, Y. Shimizu, M. Tanimoto and T. Yoshida, *Modulus τ linking leptonic CP-violation to baryon asymmetry in A_4 modular invariant flavor model*, *JHEP* **07** (2021) 184 [[arXiv:2105.14292](#)] [[INSPIRE](#)].
- [47] I. de Medeiros Varzielas and J. Lourenço, *Two A_4 modular symmetries for Tri-Maximal 2 mixing*, *Nucl. Phys. B* **979** (2022) 115793 [[arXiv:2107.04042](#)] [[INSPIRE](#)].
- [48] T. Nomura, H. Okada and Y. Orikasa, *Quark and lepton flavor model with leptiquarks in a modular A_4 symmetry*, *Eur. Phys. J. C* **81** (2021) 947 [[arXiv:2106.12375](#)] [[INSPIRE](#)].
- [49] P.T.P. Hutaauruk, D.W. Kang, J. Kim and H. Okada, *Muon $g - 2$ and neutrino mass explanations in a modular A_4 symmetry*, [arXiv:2012.11156](#) [[INSPIRE](#)].
- [50] G.-J. Ding, S.F. King and J.-N. Lu, *SO(10) models with A_4 modular symmetry*, *JHEP* **11** (2021) 007 [[arXiv:2108.09655](#)] [[INSPIRE](#)].
- [51] K.I. Nagao and H. Okada, *Modular A_4 symmetry and light dark matter with gauged $U(1)_{B-L}$* , *Phys. Dark Univ.* **36** (2022) 101039 [[arXiv:2108.09984](#)] [[INSPIRE](#)].
- [52] G. Charalampous, S.F. King, G.K. Leontaris and Y.-L. Zhou, *Flipped SU(5) with modular A_4 symmetry*, *Phys. Rev. D* **104** (2021) 115015 [[arXiv:2109.11379](#)] [[INSPIRE](#)].
- [53] H. Okada and Y.-h. Qi, *Zee-Babu model in modular A_4 symmetry*, [arXiv:2109.13779](#) [[INSPIRE](#)].
- [54] T. Nomura, H. Okada and Y.-h. Qi, *Zee model in a modular A_4 symmetry*, [arXiv:2111.10944](#) [[INSPIRE](#)].
- [55] T. Kobayashi, H. Otsuka, M. Tanimoto and K. Yamamoto, *Modular symmetry in the SMEFT*, *Phys. Rev. D* **105** (2022) 055022 [[arXiv:2112.00493](#)] [[INSPIRE](#)].
- [56] A. Dasgupta, T. Nomura, H. Okada, O. Popov and M. Tanimoto, *Dirac Radiative Neutrino Mass with Modular Symmetry and Leptogenesis*, [arXiv:2111.06898](#) [[INSPIRE](#)].
- [57] X.-G. Liu and G.-J. Ding, *Modular flavor symmetry and vector-valued modular forms*, *JHEP* **03** (2022) 123 [[arXiv:2112.14761](#)] [[INSPIRE](#)].

- [58] T. Nomura and H. Okada, *A radiative seesaw model in a supersymmetric modular A_4 group*, [arXiv:2201.10244](#) [INSPIRE].
- [59] H. Otsuka and H. Okada, *Radiative neutrino masses from modular A_4 symmetry and supersymmetry breaking*, [arXiv:2202.10089](#) [INSPIRE].
- [60] T. Nomura, H. Okada and O. Popov, *A modular A_4 symmetric scotogenic model*, *Phys. Lett. B* **803** (2020) 135294 [[arXiv:1908.07457](#)] [INSPIRE].
- [61] G. Chauhan et al., *Discrete Flavor Symmetries and Lepton Masses and Mixings*, in *2022 Snowmass Summer Study*, (2022) [[arXiv:2203.08105](#)] [INSPIRE].
- [62] S. Kikuchi, T. Kobayashi, K. Nasu, H. Otsuka, S. Takada and H. Uchida, *Modular symmetry of soft supersymmetry breaking terms*, [arXiv:2203.14667](#) [INSPIRE].
- [63] T. Kobayashi, H. Otsuka, M. Tanimoto and K. Yamamoto, *Lepton flavor violation, lepton $(g-2)_{\mu,e}$ and electron EDM in the modular symmetry*, [arXiv:2204.12325](#) [INSPIRE].
- [64] J. Gehrlein, S. Petcov, M. Spinrath and A. Titov, *Testing neutrino flavor models*, in *2022 Snowmass Summer Study*, (2022) [[arXiv:2203.06219](#)] [INSPIRE].
- [65] Y. Almumin et al., *Neutrino Flavor Model Building and the Origins of Flavor and CP Violation: A Snowmass White Paper*, in *2022 Snowmass Summer Study*, (2022) [[arXiv:2204.08668](#)] [INSPIRE].
- [66] M. Kashav and S. Verma, *On Minimal realization of Topological Lorentz Structures with one-loop Seesaw extensions in A_4 Modular Symmetry*, [arXiv:2205.06545](#) [INSPIRE].
- [67] P. Mishra, M.K. Behera, P. Panda and R. Mohanta, *Type III seesaw under A_4 modular symmetry with leptogenesis and muon $g-2$* , [arXiv:2204.08338](#) [INSPIRE].
- [68] G. Altarelli and F. Feruglio, *Discrete Flavor Symmetries and Models of Neutrino Mixing*, *Rev. Mod. Phys.* **82** (2010) 2701 [[arXiv:1002.0211](#)] [INSPIRE].
- [69] H. Ishimori, T. Kobayashi, H. Ohki, Y. Shimizu, H. Okada and M. Tanimoto, *Non-Abelian Discrete Symmetries in Particle Physics*, *Prog. Theor. Phys. Suppl.* **183** (2010) 1 [[arXiv:1003.3552](#)] [INSPIRE].
- [70] H. Ishimori, T. Kobayashi, H. Ohki, H. Okada, Y. Shimizu and M. Tanimoto, *An introduction to non-Abelian discrete symmetries for particle physicists*, *Lect. Notes Phys.* **858** (2012) 1 [INSPIRE].
- [71] D. Hernandez and A.Y. Smirnov, *Lepton mixing and discrete symmetries*, *Phys. Rev. D* **86** (2012) 053014 [[arXiv:1204.0445](#)] [INSPIRE].
- [72] S.F. King and C. Luhn, *Neutrino Mass and Mixing with Discrete Symmetry*, *Rept. Prog. Phys.* **76** (2013) 056201 [[arXiv:1301.1340](#)] [INSPIRE].
- [73] S.F. King, A. Merle, S. Morisi, Y. Shimizu and M. Tanimoto, *Neutrino Mass and Mixing: from Theory to Experiment*, *New J. Phys.* **16** (2014) 045018 [[arXiv:1402.4271](#)] [INSPIRE].
- [74] S.F. King, *Unified Models of Neutrinos, Flavour and CP-violation*, *Prog. Part. Nucl. Phys.* **94** (2017) 217 [[arXiv:1701.04413](#)] [INSPIRE].
- [75] S.T. Petcov, *Discrete Flavour Symmetries, Neutrino Mixing and Leptonic CP-violation*, *Eur. Phys. J. C* **78** (2018) 709 [[arXiv:1711.10806](#)] [INSPIRE].
- [76] T. Kobayashi, H. Ohki, H. Okada, Y. Shimizu and M. Tanimoto, *An Introduction to Non-Abelian Discrete Symmetries for Particle Physicists*, DOI (2022) [INSPIRE].

- [77] K. Ishiguro, T. Kobayashi and H. Otsuka, *Landscape of Modular Symmetric Flavor Models*, *JHEP* **03** (2021) 161 [[arXiv:2011.09154](#)] [[INSPIRE](#)].
- [78] P.P. Novichkov, J.T. Penedo, S.T. Petcov and A.V. Titov, *Generalised CP Symmetry in Modular-Invariant Models of Flavour*, *JHEP* **07** (2019) 165 [[arXiv:1905.11970](#)] [[INSPIRE](#)].
- [79] S. Kashiwase and D. Suematsu, *Baryon number asymmetry and dark matter in the neutrino mass model with an inert doublet*, *Phys. Rev. D* **86** (2012) 053001 [[arXiv:1207.2594](#)] [[INSPIRE](#)].
- [80] X. Wang and S. Zhou, *The minimal seesaw model with a modular S_4 symmetry*, *JHEP* **05** (2020) 017 [[arXiv:1910.09473](#)] [[INSPIRE](#)].
- [81] M.K. Behera and R. Mohanta, *Linear Seesaw in A'_5 Modular Symmetry With Leptogenesis*, *Front. Phys.* **10** (2022) 854595 [[arXiv:2201.10429](#)] [[INSPIRE](#)].
- [82] E. Ma, *Verifiable radiative seesaw mechanism of neutrino mass and dark matter*, *Phys. Rev. D* **73** (2006) 077301 [[hep-ph/0601225](#)] [[INSPIRE](#)].
- [83] KAMLAND-ZEN collaboration, *Search for Majorana Neutrinos near the Inverted Mass Hierarchy Region with KamLAND-Zen*, *Phys. Rev. Lett.* **117** (2016) 082503 [Addendum *ibid.* **117** (2016) 109903] [[arXiv:1605.02889](#)] [[INSPIRE](#)].
- [84] I. Esteban, M.C. Gonzalez-Garcia, A. Hernandez-Cabezudo, M. Maltoni and T. Schwetz, *Global analysis of three-flavour neutrino oscillations: synergies and tensions in the determination of θ_{23} , δ_{CP} , and the mass ordering*, *JHEP* **01** (2019) 106 [[arXiv:1811.05487](#)] [[INSPIRE](#)].
- [85] F.R. Klinkhamer and N.S. Manton, *A Saddle Point Solution in the Weinberg-Salam Theory*, *Phys. Rev. D* **30** (1984) 2212 [[INSPIRE](#)].
- [86] V.A. Kuzmin, V.A. Rubakov and M.E. Shaposhnikov, *On the Anomalous Electroweak Baryon Number Nonconservation in the Early Universe*, *Phys. Lett. B* **155** (1985) 36 [[INSPIRE](#)].